

Minimal A_4 Type-II Seesaw Realization of Testable Neutrino Mass Sum Rules

Salvador Centelles Chuliá ^{1,*} and Ranjeet Kumar ^{2,3,†}

¹*Instituto de Física Corpuscular, CSIC-Universitat de Valencia, 46980 Paterna, Spain*

²*Institute for Convergence of Basic Studies,*

Seoul National University of Science and Technology, Seoul 01811, Republic of Korea

³*Department of Physics, Indian Institute of Science Education and Research - Bhopal
Bhopal Bypass Road, Bhauri, Bhopal, India*

We propose a flavour model based on an A_4 symmetry combined with a type-II seesaw mechanism for neutrino mass generation. The resulting neutrino mass matrix obeys a sum rule that, together with the measured mass-squared differences, fully determines the absolute neutrino mass spectrum. The constrained flavour structure yields correlated predictions for lepton mixing parameters, leads to inverted ordering after imposing mixing constraints, restricts the Majorana phases and implies a neutrinoless double beta decay rate close to its maximal value for inverted ordering. In the charged lepton sector an approximate triality symmetry arises in the seesaw limit, suppressing muon flavour-violating processes and allowing only specific τ decay channels. The model provides a tightly constrained and experimentally testable framework linking neutrino masses, lepton mixing and lepton-number-violating observables.

1. INTRODUCTION

One of the open questions in the Standard Model (SM) is the pattern of fermion masses and mixings, i.e. the *flavour puzzle*. Indeed, the fermion mass pattern and quark mixing are not predicted by the theory: the Standard Model fits the observed fermion masses through Yukawa couplings, while lacking neutrino masses altogether at the renormalizable level. Discrete symmetries provide a powerful theoretical framework for alleviating the flavour puzzle by reducing the number of free parameters in the theory [1–8]. Symmetries such as the tetrahedral group A_4 [9] have been widely studied over the last two decades; see [10–27] for a selection of examples. Additionally, the breaking pattern $A_4 \rightarrow Z_3$ also leads to lepton triality [28–30], which typically imposes strong constraints on the possible signals of

* salcen@ific.uv.es

† kumarranjeet.drk@gmail.com

charged lepton flavour violation (cLFV). See [31] for a generalization of the triality residual symmetry.

Despite the phenomenological success of flavour symmetries in reproducing fermion mixing patterns, the mechanism responsible for neutrino mass generation remains unresolved. The discovery of neutrino oscillations [32, 33] provides clear evidence for physics beyond the Standard Model, most straightforwardly interpreted as the existence of non-zero neutrino masses. Among the proposed explanations, the seesaw paradigm offers a particularly compelling framework for understanding their smallness. In this work, we focus on the type-II seesaw mechanism [34–37], which does not require the introduction of new fermionic degrees of freedom beyond the Standard Model. Neutrino masses are instead generated through the vacuum expectation value of an $SU(2)_L$ scalar triplet Δ . Furthermore, the type-II seesaw can also account for the generation of the baryon asymmetry of the Universe via leptogenesis [38–43]. When combined with flavour symmetries, this framework becomes especially appealing, as it can simultaneously address the origin of neutrino masses and the observed lepton mixing patterns. The phenomenology of the type-II seesaw has been studied extensively in the literature; see, for instance, [44–47].

Another interesting aspect of flavour symmetries is the realization of neutrino mass “sum rules”. In their traditional form, these provide relations among the complex eigenvalues of the neutrino mass matrix [48–51]. More recently, mass sum rules have been derived for the singular values of the mass matrix [52, 53], which correspond directly to the physical neutrino masses rather than to its complex eigenvalues. In this framework, the experimental determination of the neutrino mass-squared differences uniquely fixes the absolute neutrino mass scale. As a consequence, the allowed parameter space relevant for beta decay and neutrinoless double beta decay ($0\nu ee$) processes is significantly constrained. This approach therefore provides a complementary probe, alongside neutrino oscillation experiments, for distinguishing among different flavour models.

In this work, we develop a simple and predictive model based on the flavour symmetry A_4 that leads to a neutrino mass sum rule and an approximate lepton triality in the charged lepton sector in the seesaw limit. Neutrino masses are generated via the type-II seesaw mechanism by introducing an $SU(2)_L$ scalar triplet Δ , which also transforms as a triplet under A_4 . The SM Higgs doublet is likewise assigned to transform as a triplet under A_4 . Its vacuum alignment $(1, 1, 1)^T$ spontaneously breaks the flavour symmetry down to its Z_3 subgroup, giving rise to lepton triality as a residual symmetry of the charged lepton sector in the seesaw limit $m_\Delta \gg \Lambda_{EW}$.

As a consequence of this structure, the charged lepton mass matrix is diagonalized by the so-called magic matrix, up to a permutation matrix. Combining the charged lepton and neutrino mixing matrices, we obtain a robust and testable correlation between the atmospheric mixing angle θ_{23} and the Dirac CP-violating phase δ_{CP} . This correlation represents a key prediction of the model and can be probed in current and future neutrino oscillation experiments. In addition, the neutrino mass sum rule fixes the absolute neutrino mass scale

once the measured mass-squared differences are imposed, leading to sharp predictions for neutrinoless double beta decay and beta decay observables. Charged lepton flavour violating processes are constrained by the approximate lepton triality.

The remainder of the paper is organized as follows. In Sec. 2, we present the field content, symmetry assignments, and vacuum alignments of the model, as well as the charged lepton and neutrino mass matrices. In Sec. 3, we derive the neutrino mass sum rule and its phenomenological consequences. In Sec. 4, we analyze the mixing predictions of the model, including neutrino oscillations, CP violation and lepton number breaking observables such as neutrinoless double beta decay. In Sec. 5 we discuss the cLFV processes allowed by the approximate triality symmetry within this model. Finally, we summarize our results and present our conclusions in Sec. 6.

2. MODEL AND FLAVOUR STRUCTURE

We consider a type-II seesaw framework with a flavor A_4 symmetry. Neutrino masses are generated from the type-II seesaw mechanism, while the A_4 symmetry fixes the structure of the neutrino mixing pattern. This framework naturally leads to neutrino mass sum rules with important implications for a variety of experiments and observations. In addition, the setup yields a rich and predictive phenomenology for cLFV. The model introduces only a single beyond the SM scalar particle, Δ , as well as promotes the Higgs doublet H into a flavour triplet. The particle content and their transformation properties under different symmetries are summarized in table I. The left handed doublet L , Higgs doublet H and triplet Δ of $SU(2)_L$ are assigned triplets under A_4 symmetry. The right handed fields l_R are singlets $(1, 1', 1'')$ under A_4 .

Fields	$SU(2)_L$	$U(1)_Y$	A_4
L	2	$-1/2$	3
l_R	1	1	1, 1'', 1'
H	2	$1/2$	3
Δ	3	1	3

TABLE I: Particle content and their transformation properties under various symmetries.

The field transformations are chosen such that the Higgs vev alignment $v(1, 1, 1)$ leads to the so-called magic matrix U_m , which diagonalizes the charged lepton mass matrix. Additionally, this vev alignment preserves a residual Z_3 symmetry after the spontaneous breaking of A_4 . This residual Z_3 symmetry has interesting phenomenological consequences for the LFV as we discuss in Sec. 5. In the neutrino sector, the vev alignment $\langle \Delta \rangle = (u_1, u_2, u_3)^T$ of the scalar triplet is responsible for the emergence of a neutrino mass sum rules. This sum rule is valid irrespective of the neutrino mass orderings. Once we impose the observed mass-squared differences constraint, this sum rule predicts the precise values for the absolute

neutrino masses. Having discussed the model framework, next we explore the neutrino mass generation and mixing.

2.1. Lagrangian and Mass Matrices

Following the charge assignment provided in table I, the invariant Yukawa Lagrangian under SM gauge symmetries and A_4 can be formulated as

$$-\mathcal{L} = \alpha_1 (\bar{L} \otimes H)_{\mathbf{1}} \otimes (l_{R_1})_{\mathbf{1}} + \alpha_2 (\bar{L} \otimes H)_{\mathbf{1}'} \otimes (l_{R_2})_{\mathbf{1}''} + \alpha_3 (\bar{L} \otimes H)_{\mathbf{1}''} \otimes (l_{R_3})_{\mathbf{1}'} + \alpha (\bar{L}^c \otimes L)_{\mathbf{3_S}} \otimes (i\tau_2 \Delta)_{\mathbf{3}} + \text{h.c.} , \quad (1)$$

where $[\dots]_{\mathbf{p}}$; $\mathbf{p} = \mathbf{1}, \mathbf{1}', \mathbf{1}'', \mathbf{3_S}, \mathbf{3}$ denote the A_4 transformation of enclosed fields. The above Lagrangian can be further expanded following the A_4 tensor product rules and given as

$$-\mathcal{L} = \alpha_1 (\bar{L}_1 H_1 + \bar{L}_2 H_2 + \bar{L}_3 H_3) l_{R_1} + \alpha_2 (\bar{L}_1 H_1 + \omega \bar{L}_2 H_2 + \omega^2 \bar{L}_3 H_3) l_{R_2} + \alpha_3 (\bar{L}_1 H_1 + \omega^2 \bar{L}_2 H_2 + \omega \bar{L}_3 H_3) l_{R_3} + \alpha [(\bar{L}_2^c L_3 + \bar{L}_3^c L_2) i\tau_2 \Delta_1 + (\bar{L}_3^c L_1 + \bar{L}_1^c L_3) i\tau_2 \Delta_2 + (\bar{L}_1^c L_2 + \bar{L}_2^c L_1) i\tau_2 \Delta_3] + \text{h.c.} . \quad (2)$$

Once the scalar fields H and Δ acquire vevs, the charged lepton and neutrino masses are generated. We focus on a particular choice for the vev alignment of these scalars. The vev alignment $\langle H \rangle = v(1, 1, 1)^T$ preserves the residual Z_3 symmetry, which have important implications for LFV processes. The choice of $\langle \Delta \rangle = (u_1, u_2, u_3)^T$ leads to the neutrino mass sum rule. From Eq. (2), the charged lepton and neutrino mass matrices can be extracted as follows

$$\mathcal{M}_l = \sqrt{3} v U_m \begin{pmatrix} \alpha_1 & 0 & 0 \\ 0 & \alpha_2 & 0 \\ 0 & 0 & \alpha_3 \end{pmatrix}, \quad \mathcal{M}_\nu = \alpha \begin{pmatrix} 0 & u_3 & u_2 \\ u_3 & 0 & u_1 \\ u_2 & u_1 & 0 \end{pmatrix} . \quad (3)$$

Where, we have defined the so-called magic matrix U_m as

$$U_m = \frac{1}{\sqrt{3}} \begin{pmatrix} 1 & 1 & 1 \\ 1 & \omega & \omega^2 \\ 1 & \omega^2 & \omega \end{pmatrix} . \quad (4)$$

We can, without loss of generality, rephase the right-handed charged leptons and the flavour triplet L to take the couplings α_i and α real and positive. Additionally, we redefine

$$\langle \Delta \rangle = u e^{i\eta_1} (\cos \theta, \sin \theta \cos \phi e^{i\eta_2}, \sin \theta \sin \phi e^{i\eta_3})^T, \quad (5)$$

where $u = \sqrt{|u_1|^2 + |u_2|^2 + |u_3|^2} > 0$, the alignment angles θ and ϕ lie in the range $[0, \pi/2]$, such that their trigonometric functions are non-negative and determine the relative alignment of the triplet vev, while the phases η_i take values in $[0, 2\pi)$.

The charged lepton mass matrix can be diagonalized as

$$U_L^\dagger \mathcal{M}_\ell U_R = \text{diag}(m_e, m_\mu, m_\tau). \quad (6)$$

Since U_m is unitary, up to permutations the only possible solution is $U_L = U_m P$, with P a permutation matrix, and $(m_e, m_\mu, m_\tau) = \sqrt{3}v (|\alpha_i|, |\alpha_j|, |\alpha_k|)$. In the neutrino sector, the mass matrix is diagonalized according to

$$U_\nu^T \mathcal{M}_\nu U_\nu = \text{diag}(m_1, m_2, m_3), \quad (7)$$

so that physical lepton mixing arises from the mismatch between the diagonalization matrices of the charged lepton and neutrino sectors and is encoded in the lepton mixing matrix, U_{\ll} , as

$$U_\ell = U_L^\dagger U_\nu. \quad (8)$$

We choose the symmetric parametrization of the lepton mixing matrix [34, 54]

$$U_{\text{lep}} = P(\delta_1, \delta_2, \delta_3) U_{23}(\theta_{23}, \phi_{23}) U_{13}(\theta_{13}, \phi_{13}) U_{12}(\theta_{12}, \phi_{12}), \quad (9)$$

where $P(\delta_1, \delta_2, \delta_3)$ is a diagonal matrix of unphysical phases and the U_{ij} are complex rotations in the ij plane, as for example,

$$U_{23}(\theta_{23}, \phi_{23}) = \begin{pmatrix} 1 & 0 & 0 \\ 0 & \cos \theta_{23} & \sin \theta_{23} e^{-i\phi_{23}} \\ 0 & -\sin \theta_{23} e^{i\phi_{23}} & \cos \theta_{23} \end{pmatrix}. \quad (10)$$

The phases ϕ_{12} and ϕ_{13} are relevant for neutrinoless double beta decay while the combination $\delta_{CP} = \phi_{13} - \phi_{12} - \phi_{23}$ is the usual Dirac CP-violating phase measured in neutrino oscillations.

We now diagonalize the lepton mass matrices and show the existence of a neutrino mass sum rule.

3. NEUTRINO MASS SUM RULE AND ABSOLUTE NEUTRINO MASS SCALE

3.1. Derivation of the sum rule

The physical neutrino masses correspond to the singular values of \mathcal{M}_ν . Therefore, the basis-invariant traces of powers of $\mathcal{M}_\nu^\dagger \mathcal{M}_\nu$ directly encode the information of the mass

spectrum. We compute the basis invariants related to the neutrino masses as [55]

$$I_{01} \equiv \text{Tr} (\mathcal{M}_\nu^\dagger \mathcal{M}_\nu) = \sum_i m_i^2 = 2\alpha^2 u^2. \quad (11)$$

$$I_{02} \equiv \text{Tr} (\mathcal{M}_\nu^\dagger \mathcal{M}_\nu \mathcal{M}_\nu^\dagger \mathcal{M}_\nu) = \sum_i m_i^4 = \frac{I_{01}^2}{2}. \quad (12)$$

$$I_{03} \equiv \text{Tr} (\mathcal{M}_\nu^\dagger \mathcal{M}_\nu \mathcal{M}_\nu^\dagger \mathcal{M}_\nu \mathcal{M}_\nu^\dagger \mathcal{M}_\nu) = \sum_i m_i^6 = \frac{I_{01}^3}{4} (1 + 6 \cos^2 \theta \sin^4 \theta \cos^2 \phi \sin^2 \phi). \quad (13)$$

As expected, the phases η_i do not affect the neutrino masses, although they will play a role in the mixing angles and CP-violating phases discussed below. The Eq. (12) implies a linear relation among the physical neutrino masses once the ordering is determined, irrespective of the choice of model parameters, i.e.

$$\sum_i m_i^4 = \frac{1}{2} \left(\sum_i m_i^2 \right)^2 \rightarrow m_3^2 = (m_2 \pm m_1)^2 \quad (14)$$

$$\Rightarrow \text{(NO): } m_3 = m_1 + m_2, \quad \text{(IO): } m_2 = m_1 + m_3. \quad (15)$$

Alternatively, irrespective of the ordering,

$$m_{\text{heaviest}} = \frac{1}{2} \sum_i m_i. \quad (16)$$

The first invariant I_{01} is completely determined by the measured mass-squared differences (Δm_{ij}^2) and the sum rule of Eq. (16). Indeed, numerically, allowing a 3σ uncertainty range for the Δm_{ij}^2 [56],

$$I_{01}^{\text{NO}} = (5.03 \pm 0.16) 10^{-3} \text{ eV}^2, \quad I_{01}^{\text{IO}} = (4.98 \pm 0.16) 10^{-3} \text{ eV}^2. \quad (17)$$

And similarly for the invariant I_{03}

$$I_{03}^{\text{NO}} = (3.88 \pm 0.09) 10^{-8} \text{ eV}^6, \quad I_{03}^{\text{IO}} = (3.08 \pm 0.07) 10^{-8} \text{ eV}^6. \quad (18)$$

Since I_{01} and I_{03} are determined for each ordering by the sum rule and the mass-squared differences, Eq. (13) gives us a restriction on θ and ϕ , leaving us with a single degree of freedom in the vev alignment of Δ , which we parametrize as t . Indeed,

$$\frac{4I_{03}}{I_{01}^3} - 1 = 6 \cos^2 \theta \sin^4 \theta \cos^2 \phi \sin^2 \phi \rightarrow (\theta(t), \phi(t)), \quad t \in [0, 1[. \quad (19)$$

At this stage, the neutrino mass spectrum is completely fixed and the alignment angles (θ, ϕ) are restricted to a one-dimensional manifold, parametrized by t . No information from lepton mixing has been used so far.

Let us do a parameter counting up to this point. In the charged lepton sector, we have 3 free parameters, α_i , which are fixed by the 3 charged lepton masses, up to a discrete choice of permutations. In the neutrino sector, there are 7 parameters (5 relevant for neutrino masses and mixings): a global factor αu , a global phase η_1 that does not affect either the neutrino masses or mixing, 2 Δ alignment angles θ and ϕ , and 2 additional phases η_2 and η_3 . Fixing the invariant I_{01} through the measured mass squared differences Δm_{21}^2 and Δm_{31}^2 determines the combination αu , while I_{02} automatically fixes the sum rule. Solving for I_{06} allows us to express θ and ϕ in terms of a single free parameter t , thus yielding the correct neutrino mass differences through Eq. (19). Finally, the 3 physical mixing angles and the 3 CP-violating phases have to be computed from the remaining 3 parameters: t , η_1 , and η_2 . Therefore, this is indeed a highly predictive flavour model, which we will discuss in Sec. 4. We now briefly summarize the possible tests of the neutrino sum rule.

3.2. Phenomenological tests of the sum rule and its predictions

We now turn to a detailed discussion of neutrino mass sum rules and their phenomenological aspects. Once Eq. (16) combined with the measured neutrino mass-squared differences [56], the sum rule fully determines the absolute neutrino mass spectrum.

NO:

$$\begin{aligned} m_3 &= m_1 + m_2, \\ \Delta m_{21}^2 &= 7.5 \times 10^{-5} \text{ eV}^2, \quad \Delta m_{31}^2 = 2.55 \times 10^{-3} \text{ eV}^2, \\ m_1 &= 0.0282 \text{ eV}, \quad m_2 = 0.0295 \text{ eV}, \quad m_3 = 0.0578 \text{ eV}. \end{aligned} \tag{20}$$

IO:

$$\begin{aligned} m_2 &= m_1 + m_3, \\ \Delta m_{21}^2 &= 7.5 \times 10^{-5} \text{ eV}^2, \quad \Delta m_{31}^2 = -2.45 \times 10^{-3} \text{ eV}^2, \\ m_3 &= 7.5 \times 10^{-4} \text{ eV}, \quad m_1 = 0.049 \text{ eV}, \quad m_2 = 0.050 \text{ eV}. \end{aligned} \tag{21}$$

This result carries important implications for several ongoing and future experiments. Cosmological observations probe the sum of neutrino masses, and it is predicted very precisely by this sum rule. Considering the mass-squared differences within their 3σ ranges,

the sum of neutrino masses is given as follows:

$$\sum_i m_i^{\text{NO}} \in [0.1138, 0.1176] \text{ eV}, \quad (22a)$$

$$\sum_i m_i^{\text{IO}} \in [0.1007, 0.1041] \text{ eV}. \quad (22b)$$

These values are compatible with the Planck 2018 results [57] as well as the latest results from the SPT-3G [58]. Its successor, the Euclid mission, is now operational and is expected to significantly improve the sensitivity to the sum of neutrino masses [59]. However, cosmological constraints on the sum of neutrino masses are dependent on the considered data-sets and cosmological models [60, 61].

Complementary constraints arise from direct neutrino mass measurements. Currently, two major experiments pursuing this approach are KATRIN [62] and Project-8 [63, 64]. The effective electron neutrino mass probed in these experiments is defined as

$$m_{\text{eff}}^{\nu_e} = \sqrt{\sum_i |U_{ei}|^2 m_i^2}. \quad (23)$$

KATRIN directly measures the effective mass of the electron neutrino and has recently reported the bound [62]

$$m_{\text{eff}}^{\nu_e} < 0.45 \text{ eV}, \quad 90\% \text{ CL (2024)}. \quad (24)$$

In contrast, the current sensitivity of Project-8 is considerably weaker than that of KATRIN, yielding the limit [63]

$$m_{\text{eff}}^{\nu_e} < 155 \text{ eV} \quad (2022). \quad (25)$$

However, future larger-volume Project-8 setups aim to reach sensitivities competitive with KATRIN, with projected reach down to a goal of $m_{\text{eff}}^{\nu_e} < 0.04 \text{ eV}$ [65]. If the mixing parameters are taken to their best fit values, the sum rule predicts

$$\text{NO: } m_{\text{eff}}^{\nu_e} = 0.028 \text{ eV}, \quad (26)$$

$$\text{IO: } m_{\text{eff}}^{\nu_e} = 0.049 \text{ eV}. \quad (27)$$

Therefore, if KATRIN or Project-8 measure a nonzero neutrino mass above these values during their runs, the model would be ruled out. Additionally, the future large volume version of Project-8 could completely probe the sum rule prediction for IO. Furthermore, this sum rule also has important consequence for the $0\nu ee$ beta decay as we discuss in Sec. 4.

Up to this point we have obtained a series of powerful analytical results that can be

extracted from the model. In what follows we perform a numerical scan over the remaining 3 free parameters t , η_2 and η_3 , as well as the discrete permutation choices in the charged lepton sector and neutrino mass ordering.

4. PREDICTIONS FOR NEUTRINO MASS ORDERING, LEPTON MIXING, CP VIOLATION AND $0\nu ee$

4.1. Normal ordering

The mixing angles predictions for the normal ordering of neutrino masses are inconsistent with the neutrino global fit [56]. Therefore, the model predicts IO of the neutrino mass. The already ongoing experiment JUNO [66] will be able to determine the ordering of neutrino masses and thus probe this model prediction. We now turn our attention to the IO.

4.2. Inverted Ordering

Continuing from Eq. (19), and allowing the mass-squared differences to vary within their 3σ ranges, we have

$$\left(\frac{4I_{03}}{I_{01}^3} - 1\right)^{\text{IO}} = (3.4 \pm 0.6) \times 10^{-4}. \quad (28)$$

Numerically scanning over t , η_1 and η_2 and fitting the lepton mixing angles on their 3σ allowed ranges, we find that the vev alignment must be a perturbation of the vacuum $(1, 1, 0)$ (and permutations), see Fig. 1. This result is purely phenomenological and follows from the interplay between the mass sum rule and the mixing constraints. The dynamical realization of such alignments is discussed in Appendix A.

The model also features a non-trivial correlation among oscillation parameters. Imposing the current 3σ allowed ranges for θ_{13} and θ_{12} , while leaving θ_{23} and the Dirac CP-violating phase δ_{CP} free, we find a strong correlation between θ_{23} and δ_{CP} , shown in the left panel of Fig. 2. Remarkably, the model predicts θ_{23} to lie close to the maximal mixing value, in good agreement with current neutrino oscillation data. Interestingly, these two parameters are currently the least precisely measured among the oscillation observables. In particular, present data show a mild tension in the preferred values of δ_{CP} as extracted by NOvA [67] and T2K [68]. The correlation predicted by the model therefore provides a clear target for future measurements. Significant progress in the determination of both θ_{23} and δ_{CP} is expected from next-generation long-baseline experiments, most notably DUNE [69] and Hyper-Kamiokande [70], which are designed to substantially reduce the uncertainties on these parameters. As a result, the θ_{23} - δ_{CP} correlation predicted here will be decisively tested in the near future.

Furthermore, there is a correlation between the CP-Violating phases of the model, two

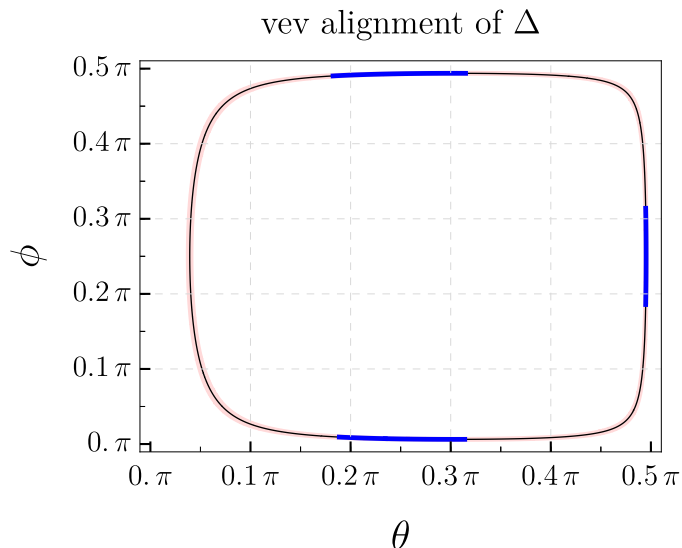


FIG. 1: Region in the (θ, ϕ) plane satisfying the neutrino mass constraints. (θ, ϕ) are the Δ vev alignment angles, see Eq. (5). The black contour corresponds to the best-fit values of the neutrino mass-squared differences [56], while the pink band shows the corresponding 3σ allowed range. The blue segments, artificially thickened for visibility, indicate the subset of solutions that are also compatible with the observed lepton mixing angles. All viable solutions lie close to the limiting vev alignments $(1, 1, 0)$, $(1, 0, 1)$, and $(0, 1, 1)$.

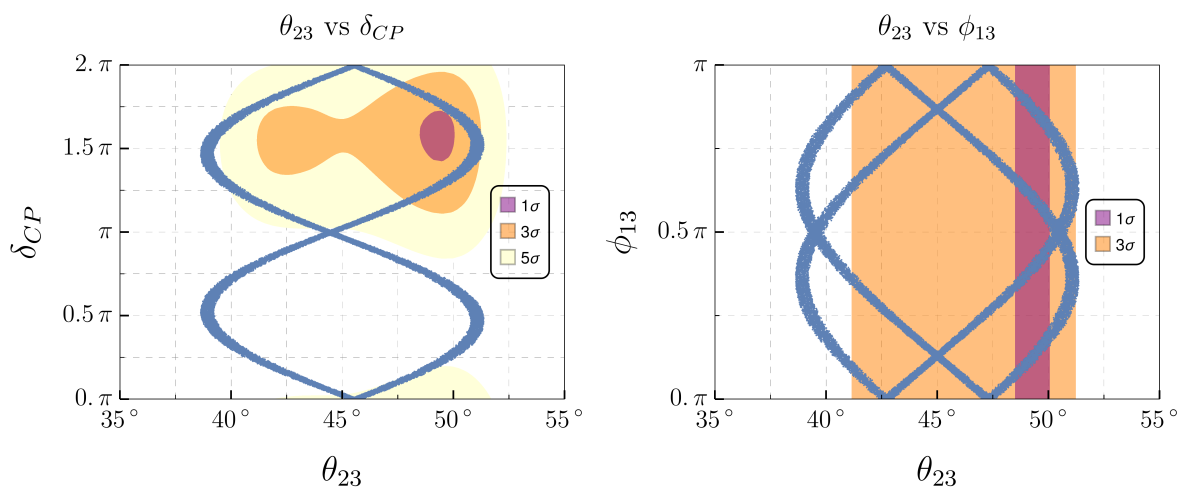


FIG. 2: Correlation of the atmospheric mixing angle θ_{23} , left panel: with the Dirac CP-violating phase δ_{CP} and right panel: Majorana phase ϕ_{13} .

of which are not experimentally determined (Majorana phases, ϕ_{12} and ϕ_{13}), and the other mixing parameters. As an example, see θ_{23} vs ϕ_{13} in Fig. 2 right panel. Additionally, ϕ_{12} is approximately restricted to 2 fixed values, see Fig. 3,

$$\phi_{12} \approx 0.11\pi \text{ or } 0.89\pi. \quad (29)$$

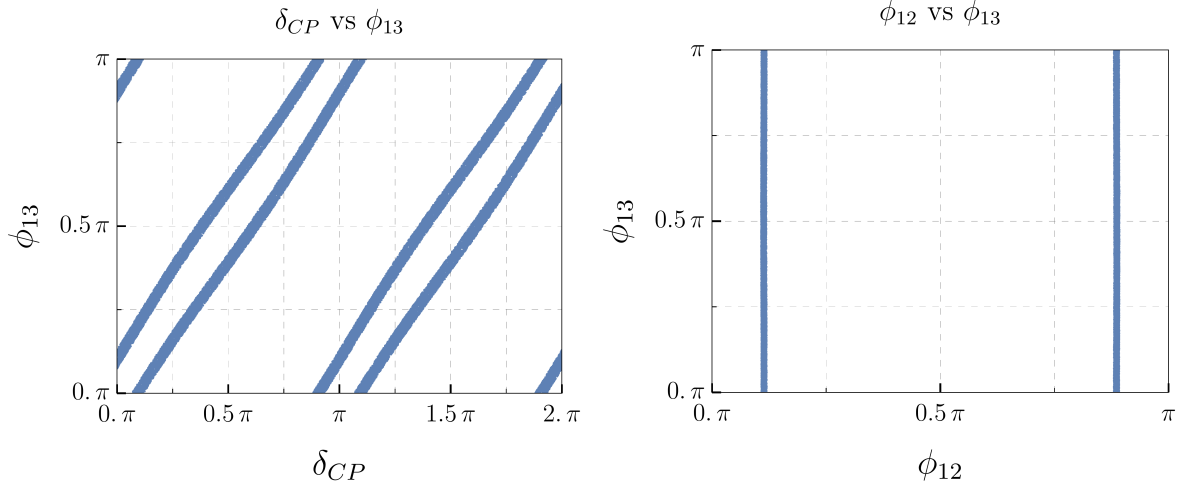


FIG. 3: Correlations between CP-violating phases. Left panel: δ_{CP} vs ϕ_{13} . Right panel: ϕ_{12} vs ϕ_{13} . Note that the Majorana phase ϕ_{12} is forced to be close to the values maximizing $|m_{ee}|$, see Eqs. (29) and (30).

This has consequences for neutrinoless beta decay experiments, since the rate of this process is proportional to the quantity $|m_{ee}|$, given by

$$|m_{ee}| = \left| \sum_i U_{ei}^2 m_i \right| = |c_{12}^2 c_{13}^2 m_1 + s_{12}^2 c_{13}^2 e^{2i\phi_{12}} m_2 + s_{13}^2 e^{2i\phi_{13}} m_3|. \quad (30)$$

For $m_3 \ll m_2, m_1$, which is the case for IO with the sum rule, Eq. (30) is maximized for $\phi_{12} = 0, \pi$. The model predicts Eq. (29), with values close to these extrema, leading to a sharply localized prediction for $|m_{ee}|$, see Fig. 4. In particular, the sharp prediction of the model is

$$|m_{ee}|^{\text{prediction}} \approx 46 \text{ meV}. \quad (31)$$

To be compared with the latest KamLAND-Zen result [71], which at 90% CL level restricts $|m_{ee}| < (28 - 122) \text{ meV}$, depending on the uncertainties of the nuclear matrix elements. The successor experiment, KamLAND-Zen2 [72] may completely rule out or confirm the model prediction.

5. CHARGED LEPTON FLAVOR VIOLATION

Charged lepton flavor-violating processes offer stringent constraints on new physics scenarios, with current experimental limits placing strong bounds on radiative and three-body decays [73]. In our model, cLFV processes are mediated by both the H and Δ flavour triplets, whose interactions generally induce flavor violation in the charged lepton sector. However, a particularly simple structure emerges in the *seesaw limit*, in which the compo-

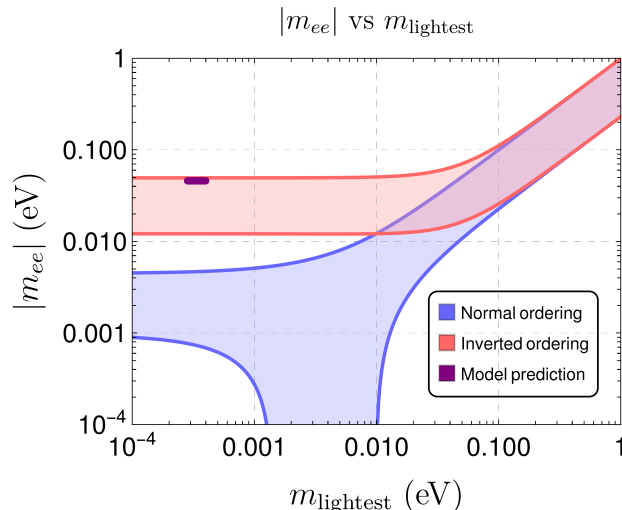


FIG. 4: Effective Majorana mass $|m_{ee}|$ as a function of the lightest neutrino mass m_{lightest} . The blue and red bands correspond to the allowed regions for normal and inverted mass ordering, respectively, obtained by varying the oscillation parameters within their current 3σ ranges. The purple band shows the prediction of the model, which enforces inverted ordering sum rule and restricts the Majorana phase ϕ_{12} (see Eq. (29)), leading to a highly localized region for $|m_{ee}|$. This results in a sharp and testable prediction for neutrinoless double beta decay experiments.

nents of Δ become heavy compared to the electroweak scale and effectively decouple. In this limit, the low-energy theory recovers a triality symmetry [28–30] that governs the remaining Higgs-mediated interactions and sharply constrains the flavor structure of cLFV processes. Throughout this section, we work in this heavy- Δ regime, where the dominant LFV effects can be analyzed in a controlled and transparent manner. To analyze the possible LFV decay rates, we first rotate the charged lepton and Higgs interaction terms given in Eq. (2) from the interaction basis to the physical mass basis. In the limit $u \ll v$, which is equivalent to $m_\nu \ll \Lambda_{EW}$, the mass matrices of H and Δ do not mix. In the mass basis, Eq. (2) can be written as follows.

$$\begin{aligned}
 \mathcal{L}_{int} = & \frac{1}{v} [m_\tau \bar{L}_\tau \tau_R + m_\mu \bar{L}_\mu \mu_R + m_e \bar{L}_e e_R] \phi_0 \\
 & + \frac{1}{v} [m_\tau \bar{L}_\mu \tau_R + m_\mu \bar{L}_e \mu_R + m_e \bar{L}_\tau e_R] \phi_1 \\
 & + \frac{1}{v} [m_\tau \bar{L}_e \tau_R + m_\mu \bar{L}_\tau \mu_R + m_e \bar{L}_\mu e_R] \phi_2 + \text{h.c.},
 \end{aligned} \tag{32}$$

where ϕ_0 , ϕ_1 , and ϕ_2 are the mass eigenstates and are related with H_1 , H_2 , and H_3 as

$$\begin{pmatrix} \phi_0 \\ \phi_1 \\ \phi_2 \end{pmatrix} = \frac{1}{\sqrt{3}} \begin{pmatrix} 1 & 1 & 1 \\ 1 & \omega & \omega^2 \\ 1 & \omega^2 & \omega \end{pmatrix} \begin{pmatrix} H_1 \\ H_2 \\ H_3 \end{pmatrix}. \tag{33}$$

The interaction term involving ϕ_0 is flavor diagonal and hence does not induce LFV processes. On the other hand, the couplings associated with ϕ_1 and ϕ_2 generate flavor off-diagonal interactions and are therefore responsible for LFV decay processes. Remarkably, all radiative two-body LFV decays, including $\mu \rightarrow e\gamma$, $\tau \rightarrow \mu\gamma$, and $\tau \rightarrow e\gamma$, are absent in this framework. As a consequence, the leading LFV signatures arise from three-body decays of the form $l_i^- \rightarrow l_j^- l_k^- l_m^+$. Among these, only the following processes are allowed:

$$\begin{aligned} \mathcal{P}_1 : \tau^- &\rightarrow \mu^- \mu^- e^+, & \mathcal{P}_2 : \tau^- &\rightarrow e^- e^- \mu^+ & (\text{mediated by } \phi_1^0) \\ \mathcal{P}_3 : \tau^- &\rightarrow e^- e^- \mu^+, & \mathcal{P}_4 : \tau^- &\rightarrow \mu^- \mu^- e^+ & (\text{mediated by } \phi_2^0) \end{aligned} \quad (34)$$

where $\phi_{1,2}^0$ are the neutral part of the scalars $\phi_{1,2}$. The Feynman diagrams for these channels have been shown in Fig. 5. The associated decay widths are proportional to $m_\tau m_\mu/v^2$ and

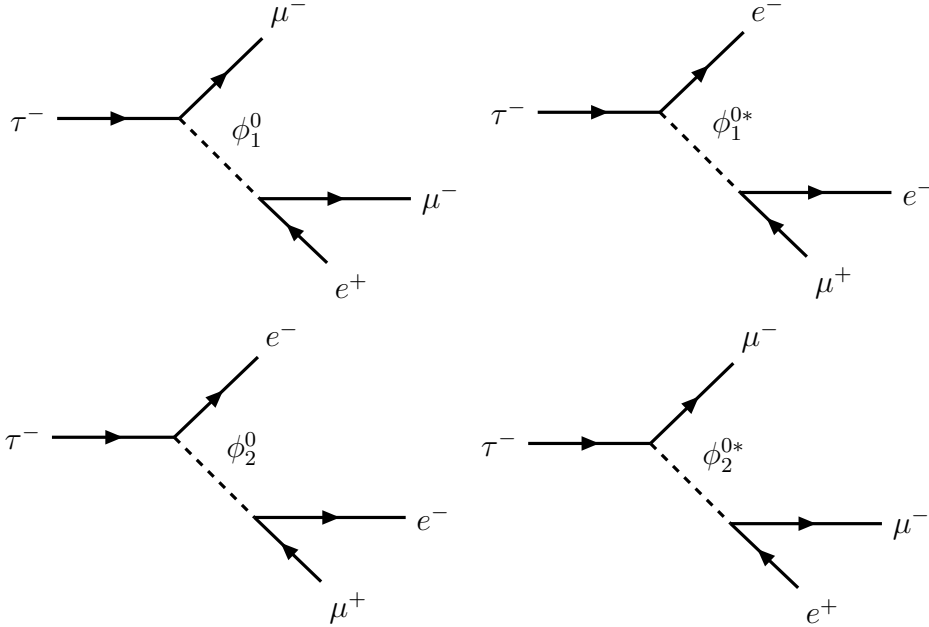


FIG. 5: Schematic Feynman diagrams of the allowed τ^- three-body decay channels mediated by the scalars ϕ_1^0 and ϕ_2^0 .

$m_e m_\mu/v^2$ for ϕ_1^0 mediation, while for ϕ_2^0 mediation they scale as $m_\tau m_e/v^2$ and $m_e m_\mu/v^2$, respectively. The decay width ($\Gamma_{\mathcal{P}_i}$) for these channels can be computed as follows:

$$\begin{aligned} \Gamma_{\mathcal{P}_1} &= \frac{1}{192\pi^3} \frac{m_\tau^5}{m_{\phi_1^0}^4} \left(\frac{m_\tau m_\mu}{v^2} \right)^2, & \Gamma_{\mathcal{P}_2} &= \frac{1}{192\pi^3} \frac{m_\tau^5}{m_{\phi_1^0}^4} \left(\frac{m_e m_\mu}{v^2} \right)^2, \\ \Gamma_{\mathcal{P}_3} &= \frac{1}{192\pi^3} \frac{m_\tau^5}{m_{\phi_2^0}^4} \left(\frac{m_\tau m_e}{v^2} \right)^2, & \Gamma_{\mathcal{P}_4} &= \frac{1}{192\pi^3} \frac{m_\tau^5}{m_{\phi_2^0}^4} \left(\frac{m_e m_\mu}{v^2} \right)^2. \end{aligned} \quad (35)$$

Since, the $\Gamma(\tau^- \rightarrow \mu^- \bar{\nu}_\mu \nu_\tau) \approx \frac{G_F^2}{192\pi^3} m_\tau^5$ (G_F is the Fermi constant), the branching ratios

(\mathcal{BR}) of these processes (\mathcal{P}_i) are given as follows:

$$\begin{aligned}
\mathcal{BR}(\mathcal{P}_1) &= \left(\frac{m_\tau m_\mu}{v^2}\right)^2 \left(\frac{1}{G_F^2 m_{\phi_1^0}^4}\right) \mathcal{BR}(\tau^- \rightarrow \mu^- \bar{\nu}_\mu \nu_\tau), \\
\mathcal{BR}(\mathcal{P}_2) &= \left(\frac{m_e m_\mu}{v^2}\right)^2 \left(\frac{1}{G_F^2 m_{\phi_1^0}^4}\right) \mathcal{BR}(\tau^- \rightarrow \mu^- \bar{\nu}_\mu \nu_\tau), \\
\mathcal{BR}(\mathcal{P}_3) &= \left(\frac{m_\tau m_e}{v^2}\right)^2 \left(\frac{1}{G_F^2 m_{\phi_2^0}^4}\right) \mathcal{BR}(\tau^- \rightarrow \mu^- \bar{\nu}_\mu \nu_\tau), \\
\mathcal{BR}(\mathcal{P}_4) &= \left(\frac{m_e m_\mu}{v^2}\right)^2 \left(\frac{1}{G_F^2 m_{\phi_2^0}^4}\right) \mathcal{BR}(\tau^- \rightarrow \mu^- \bar{\nu}_\mu \nu_\tau).
\end{aligned} \tag{36}$$

Except for \mathcal{P}_1 , all other processes are suppressed by the electron mass m_e^2 . Moreover, due to the triality symmetry, the three-body decay $\mu \rightarrow eee$ is also forbidden. The branching ratios shown above have a lower bound within the model. We focus on the dominant channel \mathcal{P}_1 . Since the electroweak scale receives contributions from multiple scalar multiplets, the vev v associated with the flavor triplet H satisfies $v < v_{SM}$. Moreover, assuming perturbative λ couplings in the scalar potential we have $m_{\phi_1^0} \lesssim v < v_{SM}$, implying

$$\mathcal{BR}(\mathcal{P}_1) = \left(\frac{m_\tau m_\mu}{v^2}\right)^2 \left(\frac{1}{G_F^2 m_{\phi_1^0}^4}\right) \mathcal{BR}(\tau^- \rightarrow \mu^- \bar{\nu}_\mu \nu_\tau) > \left(\frac{m_\tau m_\mu}{v_{SM}^2}\right)^2 \left(\frac{1}{G_F^2 v_{SM}^4}\right) \mathcal{BR}(\tau^- \rightarrow \mu^- \bar{\nu}_\mu \nu_\tau) \tag{37}$$

Using the current PDG [73] values for the charged lepton masses and electroweak parameters, we obtain the lower bound for the branching ratio of the process \mathcal{P}_1

$$\mathcal{BR}(\mathcal{P}_1) \gtrsim 10^{-12}. \tag{38}$$

While the experimental limit, also taken from the PDG, is $\mathcal{BR}(\mathcal{P}_1) < 1.7 \times 10^{-8}$. cLFV is therefore not expected to provide the leading experimental test of the model. On the other hand, triality-breaking muon decays such as $\mu \rightarrow e\gamma$ are experimentally better measured, and their detection, understood in the context of the current model, would signal a relatively low scale of the triplet Δ .

6. CONCLUSIONS

In this work, we have presented a highly predictive flavour model based on an A_4 symmetry combined with a type-II seesaw mechanism for neutrino mass generation. The flavour structure of neutrino mass matrix leads to a neutrino mass sum rule written directly in terms of the *physical* neutrino masses, understood as the singular values of the neutrino mass ma-

trix. Once the measured mass-squared differences are imposed, this sum rule completely fixes the absolute neutrino mass spectrum, independently of model parameters.

After imposing current neutrino oscillation constraints, the model also predicts *inverted neutrino mass ordering*. This feature will be robustly tested by upcoming medium-baseline reactor experiments such as JUNO, which are expected to determine the neutrino mass ordering with high significance. In addition, the sum rule leads to sharply predicted values for the effective electron neutrino mass $m_{\nu_e}^{\text{eff}}$, placing the model squarely within the reach of future direct kinematic searches. In particular, the ultimate sensitivity goals of the Project 8 experiment is expected to probe the parameter space relevant for the inverted ordering sum rule predicted here, providing a direct and model-independent test of the sum rule.

The constrained flavour structure also leads to non-trivial predictions for lepton mixing. While the solar and reactor mixing angles are imposed within their current 3σ ranges, the atmospheric mixing angle θ_{23} and the Dirac CP-violating phase δ_{CP} emerge as correlated predictions of the model. Remarkably, θ_{23} is predicted to lie close to maximal mixing, in good agreement with present data. Since θ_{23} and δ_{CP} are currently the least precisely measured oscillation parameters, the predicted correlation provides a clear and testable target for next-generation long-baseline experiments, such as DUNE and Hyper-Kamiokande.

The model further predicts a highly localized region for the effective Majorana mass $|m_{ee}|$ governing neutrinoless double beta decay. Due to the restricted values of the Majorana phases enforced by the flavour structure, the predicted $|m_{ee}|$ lies close to its maximal value for inverted ordering. Interestingly, the current KamLAND-Zen limits already probe part of this region, although dominated by uncertainties in the nuclear matrix elements. The upcoming KamLAND-Zen2 experiment is therefore expected to play a decisive role in either confirming or ruling out this prediction.

Finally, charged lepton flavour violation provides a complementary probe of the model. In the seesaw limit, where the scalar triplet Δ is heavy and decoupled, the low-energy theory exhibits lepton triality, leading to the absence of muon flavour-violating decays, while allowing specific three-body τ decays. Although the predicted τ decay rates lie well below current experimental sensitivities, the observation of triality-breaking processes such as $\mu \rightarrow e\gamma$ or $\mu \rightarrow eee$ would provide indirect evidence for a relatively low scale of the triplet Δ , offering an alternative window into the ultraviolet completion of the model.

The model yields a set of predictions for neutrino mass ordering, absolute neutrino mass measurements, CP violation, neutrinoless double beta decay and charged lepton flavour violation. The convergence of multiple experimental frontiers in the coming years therefore makes this framework both highly constrained and testable.

ACKNOWLEDGMENTS

SCCh acknowledges support from the Spanish grants PID2023-147306NB-I00, CNS2024-154524 and CEX2023-001292-S (MICIU/AEI/10.13039/501100011033). RK would like to acknowledge support from the Research Program funded by the Seoul National University of Science and Technology. We would also like to thank the organizers of the FLASY 2025 conference in Rome, where this project was initiated.

Appendix A: Scalar Sector and Mass Spectrum

The scalar sector of the model contains a $SU(2)_L$ doublet Higgs H and a triplet Δ , both of which are triplets under the A_4 flavor symmetry. In addition, a separate Higgs doublet H_q , singlet under A_4 , is introduced to generate the quark masses. Since H_q does not participate in the flavor dynamics discussed in this work, it does not play any role in the scalar potential relevant for the lepton sector and will not be discussed further. The scalar potential invariant under the SM gauge group and A_4 can be formulated as follows [74]:

$$\begin{aligned}
V = & -m_H^2 \left(H_1^\dagger H_1 + H_2^\dagger H_2 + H_3^\dagger H_3 \right) + \lambda_{H1} \left(H_1^\dagger H_1 + H_2^\dagger H_2 + H_3^\dagger H_3 \right)^2 \\
& + \lambda_{H2} \left[\left(H_1^\dagger H_1 \right) \left(H_2^\dagger H_2 \right) + \left(H_2^\dagger H_2 \right) \left(H_3^\dagger H_3 \right) + \left(H_3^\dagger H_3 \right) \left(H_1^\dagger H_1 \right) \right] \\
& + \lambda_{H3} \left(|H_1^\dagger H_2|^2 + |H_2^\dagger H_3|^2 + |H_3^\dagger H_1|^2 \right) + \lambda_{H4} \left[\left(H_1^\dagger H_2 \right)^2 + \left(H_2^\dagger H_3 \right)^2 + \left(H_3^\dagger H_1 \right)^2 + \text{h.c.} \right] \\
& - M_\Delta'^2 \text{Tr} \left[\left(\Delta_1^\dagger \Delta_1 + \Delta_2^\dagger \Delta_2 + \Delta_3^\dagger \Delta_3 \right) \right] + \lambda_{\Delta 0} \left(\text{Tr} \left[\Delta_1^\dagger \Delta_1 + \Delta_2^\dagger \Delta_2 + \Delta_3^\dagger \Delta_3 \right] \right)^2 \\
& + \lambda_{\Delta 1} \text{Tr} \left[\left(\Delta_1^\dagger \Delta_1 + \Delta_2^\dagger \Delta_2 + \Delta_3^\dagger \Delta_3 \right)^2 \right] \\
& + \lambda_{\Delta 2} \text{Tr} \left[\left(\Delta_1^\dagger \Delta_1 \right) \left(\Delta_2^\dagger \Delta_2 \right) + \left(\Delta_2^\dagger \Delta_2 \right) \left(\Delta_3^\dagger \Delta_3 \right) + \left(\Delta_3^\dagger \Delta_3 \right) \left(\Delta_1^\dagger \Delta_1 \right) \right] \\
& + \lambda_{\Delta 3} \text{Tr} \left[|\Delta_1^\dagger \Delta_2|^2 + |\Delta_2^\dagger \Delta_3|^2 + |\Delta_3^\dagger \Delta_1|^2 \right] + \lambda_{\Delta 4} \text{Tr} \left[\left(\Delta_1^\dagger \Delta_2 \right)^2 + \left(\Delta_2^\dagger \Delta_3 \right)^2 + \left(\Delta_3^\dagger \Delta_1 \right)^2 + \text{h.c.} \right] \\
& + \lambda_{H\Delta 1} \left(H_1^\dagger H_1 + H_2^\dagger H_2 + H_3^\dagger H_3 \right) \text{Tr} \left[\left(\Delta_1^\dagger \Delta_1 + \Delta_2^\dagger \Delta_2 + \Delta_3^\dagger \Delta_3 \right) \right] \\
& + \lambda_{H\Delta 2} \left[\left(H_1^\dagger \Delta_2 \right) \left(\Delta_2^\dagger H_1 \right) + \left(H_2^\dagger \Delta_3 \right) \left(\Delta_3^\dagger H_2 \right) + \left(H_3^\dagger \Delta_1 \right) \left(\Delta_1^\dagger H_3 \right) \right] \\
& + \lambda_{H\Delta 3} \left[\left(H_1^\dagger \Delta_2 \right) \left(\Delta_1^\dagger H_2 \right) + \left(H_2^\dagger \Delta_3 \right) \left(\Delta_2^\dagger H_3 \right) + \left(H_3^\dagger \Delta_1 \right) \left(\Delta_3^\dagger H_1 \right) + \text{h.c.} \right] \\
& + \kappa_1 \left(H_1^T \tilde{\Delta}_2^\dagger H_3 + H_2^T \tilde{\Delta}_3^\dagger H_1 + H_3^T \tilde{\Delta}_1^\dagger H_2 + \text{h.c.} \right) + \kappa_2 \left(H_1^T \tilde{\Delta}_3^\dagger H_2 + H_2^T \tilde{\Delta}_1^\dagger H_3 + H_3^T \tilde{\Delta}_2^\dagger H_1 + \text{h.c.} \right) .
\end{aligned} \tag{A1}$$

where $\tilde{\Delta}_i \equiv i\tau_2 \Delta_i$. As discussed in Sec. 4, all viable solution for the vev alignment of Δ are close to $u_i = u_j = u'$, $u_k = 0$. Thus the tadpole solutions with this approximation are given

by

$$\begin{aligned}\mu_H^2 &= (3\lambda_{H1} + \lambda_{H2} + \lambda_{H3} + 2\lambda_{H4})v^2 + \frac{1}{2}(2\lambda_{H\Delta1} + \lambda_{H\Delta2} + \lambda_{H\Delta3})u'^2 - \frac{\kappa_1 + \kappa_2}{\sqrt{2}}u', \\ M_\Delta'^2 &= (2\lambda_{\Delta0} + 2\lambda_{\Delta1} + \frac{\lambda_{\Delta2}}{2} + \frac{\lambda_{\Delta3}}{2} + \lambda_{\Delta4})u'^2 + \frac{1}{2}(3\lambda_{H\Delta1} + \lambda_{H\Delta2} + \lambda_{H\Delta3})v^2 - \frac{\kappa_1 + \kappa_2}{\sqrt{2}u'}v^2.\end{aligned}\tag{A2}$$

The exact alignment $(u, u, 0)$ follows from the scalar potential in Eq. (A1). Small deviations from this configuration, required to reproduce the phenomenologically viable alignment discussed in Sec. 4, can be obtained by introducing soft A_4 -breaking terms in the scalar potential of the form $\mu_{ij} \Delta_i^\dagger \Delta_j$. These terms do not affect the structure of the Yukawa sector discussed in the main text and can naturally be taken small, ensuring that the alignment remains close to the symmetric configuration.

In the limit $u \ll v$, the Higgs mass squared matrix effectively decouples from the Δ mass squared matrix and can be written as

$$\mathcal{M}_H^2 = v^2 \begin{pmatrix} a & a+b & a+b \\ a+b & a & a+b \\ a+b & a+b & a \end{pmatrix}.\tag{A3}$$

The eigenvalues of this matrix are as follows

$$m_h^2 = (3a + 2b)v^2, \quad m_{h_2, h_3}^2 = -bv^2,\tag{A4}$$

where $a \equiv 2\lambda_{H1}$ and $b \equiv \lambda_{H2} + \lambda_{H3} + 2\lambda_{H4}$. The bounded from below (BFB) condition for Higgs potential is given by [74]

$$\begin{aligned}\lambda_{H1} &\geq 0, & 3\lambda_{H1} + \lambda_{H2} + \lambda_{H3} + 2\lambda_{H4} &\geq 0, \\ 3\lambda_{H1} + \lambda_{H2} + \lambda_{H3} - \lambda_{H4} &\geq 0, & 4\lambda_{H1} + \lambda_{H2} + \lambda_{H3} - 2\lambda_{H4} &\geq 0.\end{aligned}\tag{A5}$$

-
- [1] K. S. Babu and R. N. Mohapatra, ‘‘Permutation Symmetry and the Origin of Fermion Mass Hierarchy,’’ *Phys. Rev. Lett.* **64** (1990) 2747.
- [2] P. H. Frampton and T. W. Kephart, ‘‘Simple nonAbelian finite flavor groups and fermion masses,’’ *Int. J. Mod. Phys. A* **10** (1995) 4689–4704, [arXiv:hep-ph/9409330](#).
- [3] J. Kubo, A. Mondragon, M. Mondragon, and E. Rodriguez-Jauregui, ‘‘The Flavor symmetry,’’ *Prog. Theor. Phys.* **109** (2003) 795–807, [arXiv:hep-ph/0302196](#). [Erratum: *Prog.Theor.Phys.* 114, 287–287 (2005)].

- [4] G. Altarelli and F. Feruglio, “Discrete Flavor Symmetries and Models of Neutrino Mixing,” *Rev. Mod. Phys.* **82** (2010) 2701–2729, [arXiv:1002.0211 \[hep-ph\]](#).
- [5] S. Morisi and J. W. F. Valle, “Neutrino masses and mixing: a flavour symmetry roadmap,” *Fortsch.Phys.* **61** (2013) 466–492, [arXiv:1206.6678 \[hep-ph\]](#).
- [6] F. Feruglio and A. Romanino, “Lepton flavor symmetries,” *Rev.Mod.Phys.* **93** (2021) 015007, [arXiv:1912.06028 \[hep-ph\]](#).
- [7] P. B. Denton and J. Gehrlein, “Survey of neutrino flavor predictions and the neutrinoless double beta decay funnel,” *Phys. Rev. D* **109** no. 5, (2024) 055028, [arXiv:2308.09737 \[hep-ph\]](#).
- [8] G.-J. Ding and J. W. F. Valle, “The symmetry approach to quark and lepton masses and mixing,” *Phys. Rept.* **1109** (2025) 1–105, [arXiv:2402.16963 \[hep-ph\]](#).
- [9] H. Ishimori *et al.*, “Non-Abelian Discrete Symmetries in Particle Physics,” *Prog.Theor.Phys.Suppl.* **183** (2010) 1–163, [arXiv:1003.3552 \[hep-th\]](#).
- [10] K. Babu, E. Ma, and J. W. F. Valle, “Underlying $A(4)$ symmetry for the neutrino mass matrix and the quark mixing matrix,” *Phys.Lett.* **B552** (2003) 207–213.
- [11] S.-L. Chen, M. Frigerio, and E. Ma, “Hybrid seesaw neutrino masses with $A(4)$ family symmetry,” *Nucl. Phys. B* **724** (2005) 423–431, [arXiv:hep-ph/0504181](#).
- [12] G. Altarelli and F. Feruglio, “Tri-bimaximal neutrino mixing, $A(4)$ and the modular symmetry,” *Nucl. Phys. B* **741** (2006) 215–235, [arXiv:hep-ph/0512103](#).
- [13] A. E. Carcamo Hernandez, I. de Medeiros Varzielas, S. G. Kovalenko, H. Päs, and I. Schmidt, “Lepton masses and mixings in an A_4 multi-Higgs model with a radiative seesaw mechanism,” *Phys. Rev. D* **88** no. 7, (2013) 076014, [arXiv:1307.6499 \[hep-ph\]](#).
- [14] A. E. Cárcamo Hernández and R. Martinez, “A predictive 3-3-1 model with A_4 flavor symmetry,” *Nucl. Phys. B* **905** (2016) 337–358, [arXiv:1501.05937 \[hep-ph\]](#).
- [15] D. Borah and B. Karmakar, “ A_4 flavour model for Dirac neutrinos: Type I and inverse seesaw,” *Phys. Lett. B* **780** (2018) 461–470, [arXiv:1712.06407 \[hep-ph\]](#).
- [16] A. E. Cárcamo Hernández and H. N. Long, “A highly predictive A_4 flavour 3-3-1 model with radiative inverse seesaw mechanism,” *J. Phys. G* **45** no. 4, (2018) 045001, [arXiv:1705.05246 \[hep-ph\]](#).
- [17] S. Centelles Chuliá, R. Srivastava, and J. W. F. Valle, “Generalized Bottom-Tau unification, neutrino oscillations and dark matter: predictions from a lepton quarticity flavor approach,” *Phys.Lett.* **B773** (2017) 26–33, [arXiv:1706.00210 \[hep-ph\]](#).
- [18] D. Borah and B. Karmakar, “Linear seesaw for Dirac neutrinos with A_4 flavour symmetry,” *Phys. Lett. B* **789** (2019) 59–70, [arXiv:1806.10685 \[hep-ph\]](#).
- [19] G.-J. Ding, J.-N. Lu, and J. W. F. Valle, “Trimaximal neutrino mixing from scotogenic A_4 family symmetry,” *Phys. Lett. B* **815** (2021) 136122, [arXiv:2009.04750 \[hep-ph\]](#).
- [20] R. Kumar, P. Mishra, M. K. Behera, R. Mohanta, and R. Srivastava, “Predictions from scoto-seesaw with A_4 modular symmetry,” *Phys. Lett. B* **853** (2024) 138635,

- [arXiv:2310.02363 \[hep-ph\]](#).
- [21] S. Mahapatra, S. K. Sahoo, N. Sahu, and V. S. Thounaojam, “Self-interacting dark matter and Dirac neutrinos via lepton quarticity,” *Phys. Rev. D* **109** no. 5, (2024) 055036, [arXiv:2312.12322 \[hep-ph\]](#).
- [22] L. Singh, M. Kashav, and S. Verma, “Minimal type-I Dirac seesaw and leptogenesis under A_4 modular invariance,” *Nucl. Phys. B* **1007** (2024) 116666, [arXiv:2405.07165 \[hep-ph\]](#).
- [23] T. Nomura and H. Okada, “Type-II seesaw of a non-holomorphic modular A_4 symmetry,” *Phys. Lett. B* **868** (2025) 139763, [arXiv:2408.01143 \[hep-ph\]](#).
- [24] A. Palavrić, “Discrete leptonic flavor symmetries: UV mediators and phenomenology,” *Phys. Rev. D* **110** no. 11, (2024) 115025, [arXiv:2408.16044 \[hep-ph\]](#).
- [25] G. Pathak, P. Das, and M. K. Das, “Neutrino mass genesis in scoto-inverse seesaw with modular A_4 ,” *Eur. Phys. J. C* **85** no. 5, (2025) 569, [arXiv:2411.13895 \[hep-ph\]](#).
- [26] A. Moreno-Sánchez and A. Palavrić, “Leptonic flavor from a modular A_4 symmetry: UV mediators and SMEFT realizations,” *Phys. Rev. D* **112** no. 7, (2025) 075002, [arXiv:2505.01535 \[hep-ph\]](#).
- [27] S. T. Goswami and S. Roy, “Permuted Charged Lepton Correction in the Framework of Dirac Seesaw,” [arXiv:2501.18181 \[hep-ph\]](#).
- [28] E. Ma and G. Rajasekaran, “Softly broken $A(4)$ symmetry for nearly degenerate neutrino masses,” *Phys. Rev. D* **64** (2001) 113012, [arXiv:hep-ph/0106291](#).
- [29] E. Ma, “Quark and Lepton Flavor Triality,” *Phys. Rev. D* **82** (2010) 037301, [arXiv:1006.3524 \[hep-ph\]](#).
- [30] Q.-H. Cao, A. Damanik, E. Ma, and D. Wegman, “Probing Lepton Flavor Triality with Higgs Boson Decay,” *Phys. Rev. D* **83** (2011) 093012, [arXiv:1103.0008 \[hep-ph\]](#).
- [31] L. Calibbi, C. Hagedorn, M. A. Schmidt, and J. Vandelev, “Selection rules for charged lepton flavour violating processes from residual flavour groups,” [arXiv:2505.24350 \[hep-ph\]](#).
- [32] T. Kajita, “Nobel Lecture: Discovery of atmospheric neutrino oscillations,” *Rev. Mod. Phys.* **88** no. 3, (2016) 030501.
- [33] A. B. McDonald, “Nobel Lecture: The Sudbury Neutrino Observatory: Observation of flavor change for solar neutrinos,” *Rev. Mod. Phys.* **88** (2016) 030502.
- [34] J. Schechter and J. W. F. Valle, “Neutrino Masses in $SU(2) \times U(1)$ Theories,” *Phys. Rev. D* **22** (1980) 2227.
- [35] M. Magg and C. Wetterich, “Neutrino Mass Problem and Gauge Hierarchy,” *Phys. Lett. B* **94** (1980) 61–64.
- [36] T. P. Cheng and L.-F. Li, “Neutrino Masses, Mixings and Oscillations in $SU(2) \times U(1)$ Models of Electroweak Interactions,” *Phys. Rev. D* **22** (1980) 2860.
- [37] R. N. Mohapatra and G. Senjanovic, “Neutrino Masses and Mixings in Gauge Models with Spontaneous Parity Violation,” *Phys. Rev. D* **23** (1981) 165.

- [38] E. Ma and U. Sarkar, “Neutrino masses and leptogenesis with heavy Higgs triplets,” *Phys. Rev. Lett.* **80** (1998) 5716–5719, [arXiv:hep-ph/9802445](#).
- [39] S. Antusch and S. F. King, “Type II Leptogenesis and the neutrino mass scale,” *Phys. Lett. B* **597** (2004) 199–207, [arXiv:hep-ph/0405093](#).
- [40] S. Antusch, “Flavour-dependent type II leptogenesis,” *Phys. Rev. D* **76** (2007) 023512, [arXiv:0704.1591 \[hep-ph\]](#).
- [41] N. D. Barrie, C. Han, and H. Murayama, “Affleck-Dine Leptogenesis from Higgs Inflation,” *Phys. Rev. Lett.* **128** no. 14, (2022) 141801, [arXiv:2106.03381 \[hep-ph\]](#).
- [42] N. D. Barrie, C. Han, and H. Murayama, “Type II Seesaw leptogenesis,” *JHEP* **05** (2022) 160, [arXiv:2204.08202 \[hep-ph\]](#).
- [43] M. Berbig, “Type II Seesaw Leptogenesis in a Majoron background,” [arXiv:2506.23290 \[hep-ph\]](#).
- [44] L. Lavoura, “General formulae for $f(1) \rightarrow f(2) \gamma$,” *Eur. Phys. J. C* **29** (2003) 191–195, [arXiv:hep-ph/0302221](#).
- [45] D. N. Dinh, A. Ibarra, E. Molinaro, and S. T. Petcov, “The $\mu - e$ Conversion in Nuclei, $\mu \rightarrow e\gamma$, $\mu \rightarrow 3e$ Decays and TeV Scale See-Saw Scenarios of Neutrino Mass Generation,” *JHEP* **08** (2012) 125, [arXiv:1205.4671 \[hep-ph\]](#). [Erratum: *JHEP* 09, 023 (2013)].
- [46] N. D. Barrie and S. T. Petcov, “Lepton Flavour Violation tests of Type II Seesaw Leptogenesis,” *JHEP* **01** (2023) 001, [arXiv:2210.02110 \[hep-ph\]](#).
- [47] S. Mandal, O. G. Miranda, G. Sanchez Garcia, J. W. F. Valle, and X.-J. Xu, “Toward deconstructing the simplest seesaw mechanism,” *Phys. Rev. D* **105** no. 9, (2022) 095020, [arXiv:2203.06362 \[hep-ph\]](#).
- [48] J. Barry and W. Rodejohann, “Neutrino Mass Sum-rules in Flavor Symmetry Models,” *Nucl. Phys. B* **842** (2011) 33–50, [arXiv:1007.5217 \[hep-ph\]](#).
- [49] S. F. King, A. Merle, and A. J. Stuart, “The Power of Neutrino Mass Sum Rules for Neutrinoless Double Beta Decay Experiments,” *JHEP* **12** (2013) 005, [arXiv:1307.2901 \[hep-ph\]](#).
- [50] J. Gehrlein, A. Merle, and M. Spinrath, “Predictivity of Neutrino Mass Sum Rules,” *Phys. Rev. D* **94** no. 9, (2016) 093003, [arXiv:1606.04965 \[hep-ph\]](#).
- [51] J. Gehrlein and M. Spinrath, “Leptonic Sum Rules from Flavour Models with Modular Symmetries,” *JHEP* **03** (2021) 177, [arXiv:2012.04131 \[hep-ph\]](#).
- [52] S. Chuliá Centelles, R. Cepedello, and O. Medina, “Absolute neutrino mass scale and dark matter stability from flavour symmetry,” *JHEP* **10** (2022) 080, [arXiv:2204.12517 \[hep-ph\]](#).
- [53] S. Centelles Chuliá, R. Kumar, O. Popov, and R. Srivastava, “Neutrino mass sum rules from modular A_4 symmetry,” *Phys. Rev. D* **109** no. 3, (2024) 035016, [arXiv:2308.08981 \[hep-ph\]](#).
- [54] W. Rodejohann and J. W. F. Valle, “Symmetrical Parametrizations of the Lepton Mixing

- Matrix,” *Phys.Rev.* **D84** (2011) 073011, [arXiv:1108.3484 \[hep-ph\]](#).
- [55] M. P. Bento, J. P. Silva, and A. Trautner, “The basis invariant flavor puzzle,” *JHEP* **01** (2024) 024, [arXiv:2308.00019 \[hep-ph\]](#).
- [56] P. F. de Salas, D. V. Forero, S. Gariazzo, P. Martínez-Miravé, O. Mena, C. A. Ternes, M. Tórtola, and J. W. F. Valle, “2020 global reassessment of the neutrino oscillation picture,” *JHEP* **02** (2021) 071, [arXiv:2006.11237 \[hep-ph\]](#).
- [57] **Planck** Collaboration, N. Aghanim *et al.*, “Planck 2018 results. VI. Cosmological parameters,” *Astron. Astrophys.* **641** (2020) A6, [arXiv:1807.06209 \[astro-ph.CO\]](#). [Erratum: *Astron.Astrophys.* 652, C4 (2021)].
- [58] **SPT-3G** Collaboration, E. Camphuis *et al.*, “SPT-3G D1: CMB temperature and polarization power spectra and cosmology from 2019 and 2020 observations of the SPT-3G Main field,” [arXiv:2506.20707 \[astro-ph.CO\]](#).
- [59] L. Amendola *et al.*, “Cosmology and fundamental physics with the Euclid satellite,” *Living Rev. Rel.* **21** no. 1, (2018) 2, [arXiv:1606.00180 \[astro-ph.CO\]](#).
- [60] T. Bertólez-Martínez, I. Esteban, R. Hajjar, O. Mena, and J. Salvado, “Origin of cosmological neutrino mass bounds: background versus perturbations,” *JCAP* **06** (2025) 058, [arXiv:2411.14524 \[astro-ph.CO\]](#).
- [61] D. Naredo-Tuero, M. Escudero, E. Fernández-Martínez, X. Marcano, and V. Poulin, “Critical look at the cosmological neutrino mass bound,” *Phys. Rev. D* **110** no. 12, (2024) 123537, [arXiv:2407.13831 \[astro-ph.CO\]](#).
- [62] **KATRIN** Collaboration, M. Aker *et al.*, “Direct neutrino-mass measurement based on 259 days of KATRIN data,” *Science* **388** no. 6743, (2025) adq9592, [arXiv:2406.13516 \[nucl-ex\]](#).
- [63] **Project 8** Collaboration, A. Ashtari Esfahani *et al.*, “Tritium Beta Spectrum Measurement and Neutrino Mass Limit from Cyclotron Radiation Emission Spectroscopy,” *Phys. Rev. Lett.* **131** no. 10, (2023) 102502, [arXiv:2212.05048 \[nucl-ex\]](#).
- [64] **Project 8** Collaboration, A. Ashtari Esfahani *et al.*, “Antenna arrays for neutrino mass measurements with cyclotron radiation emission spectroscopy,” *Phys. Rev. C* **112** no. 4, (2025) 045506.
- [65] **Project 8** Collaboration, A. A. Esfahani *et al.*, “The Project 8 Neutrino Mass Experiment,” in *Snowmass 2021*. 3, 2022. [arXiv:2203.07349 \[nucl-ex\]](#).
- [66] **JUNO** Collaboration, A. Abusleme *et al.*, “First measurement of reactor neutrino oscillations at JUNO,” [arXiv:2511.14593 \[hep-ex\]](#).
- [67] **NOvA** Collaboration, M. A. Acero *et al.*, “Improved measurement of neutrino oscillation parameters by the NOvA experiment,” *Phys. Rev. D* **106** no. 3, (2022) 032004, [arXiv:2108.08219 \[hep-ex\]](#).
- [68] **T2K** Collaboration, K. Abe *et al.*, “Measurements of neutrino oscillation parameters from the T2K experiment using 3.6×10^{21} protons on target,” *Eur. Phys. J. C* **83** no. 9, (2023)

- 782, [arXiv:2303.03222 \[hep-ex\]](#).
- [69] **DUNE** Collaboration, B. Abi *et al.*, “Deep Underground Neutrino Experiment (DUNE), Far Detector Technical Design Report, Volume II: DUNE Physics,” [arXiv:2002.03005 \[hep-ex\]](#).
- [70] **Hyper-Kamiokande** Collaboration, K. Abe *et al.*, “Hyper-Kamiokande Design Report,” [arXiv:1805.04163 \[physics.ins-det\]](#).
- [71] **KamLAND-Zen** Collaboration, S. Abe *et al.*, “Search for Majorana Neutrinos with the Complete KamLAND-Zen Dataset,” [arXiv:2406.11438 \[hep-ex\]](#).
- [72] J. Nakane, “New detector development and performance evaluation for KamLAND2-Zen experiment,” *Nucl. Instrum. Meth. A* **1081** (2026) 170850.
- [73] **Particle Data Group** Collaboration, S. Navas *et al.*, “Review of particle physics,” *Phys. Rev. D* **110** no. 3, (2024) 030001.
- [74] N. Buskin and I. P. Ivanov, “Bounded-from-below conditions for A_4 -symmetric 3HDM,” *J. Phys. A* **54** (2021) 325401, [arXiv:2104.11428 \[hep-ph\]](#).